



Contributions of Long-Range Transported and Locally Emitted Nitrate in Size-Segregated Aerosols in Japan at Kyushu and Okinawa

Shiori Tatsuta¹, Kojiro Shimada², Chak K. Chan³, Yong Pyo Kim^{2,4}, Neng-Huei Lin^{2,5}, Akinori Takami⁶, Shiro Hatakeyama^{1,2,7*}

¹ Graduate School of Agriculture, Tokyo University of Agriculture and Technology, Fuchu, Tokyo 183-8509, Japan

² Global Innovation Research Organization, Tokyo University of Agriculture and Technology, Fuchu, Tokyo 183-8538, Japan

³ School of Energy and Environment, City University of Hong Kong, Hong Kong, China

⁴ Department of Environmental Science & Engineering and Department of Chemical, Engineering & Materials Science, Ewha Womans University, Seoul 03760, Korea

⁵ Department of Atmospheric Sciences and Department of Chemistry, National Central University, Chung-Li, Taoyuan 32001, Taiwan

⁶ National Institute for Environmental Studies, Tsukuba, Ibaraki 305-8506, Japan

⁷ Center for Environmental Science in Saitama, Kazo, Saitama 347-0115, Japan

ABSTRACT

We observed the size distributions of mass concentration, ionic composition, and trace metal concentration in aerosols collected at an urban site in Kumamoto Prefecture (KM) and a rural site at Cape Hedo in Okinawa Prefecture (HD) between 2012 and 2015. To evaluate the contribution of transboundary nitrate and locally emitted nitrate in the aerosols at Kumamoto, we distinguished between days of transboundary air pollution from East Asia and days of local air pollution on the basis of a threshold for Pb concentration and the ratio Pb (in $0.5 < \text{projected area diameter (Dp)} < 1.0 \mu\text{m}$)/Cu (in $2.5 < \text{Dp} < 10 \mu\text{m}$). Fine nitrate (particulate NH_4NO_3) did not arrive at HD from the Asian continent even under long-range transport conditions. Fine nitrate emitted in Kumamoto and its vicinity also was not transported to HD, even in an air mass that passed over KM and reached HD within one day. Almost all fine nitrate was converted to coarse nitrate during transport by dissociation of fine nitrate and adsorption of HNO_3 on larger aerosol particles. Transboundary nitrate existed largely in the particle size range of $0.5 < \text{Dp} < 10 \mu\text{m}$, and the contribution of transboundary nitrate in the particle size range of $0.1 < \text{Dp} < 0.5 \mu\text{m}$ was about 20% even under long-range transport conditions. The contribution of transboundary nitrate in particles with $\text{Dp} < 2.5 \mu\text{m}$ at KM was approximately 50%, 50%, and 80% in spring, autumn, and winter, respectively.

Keywords: Nitrate; Transport of fine nitrate; East Asia; Contribution of long-range transport and local air pollution.

INTRODUCTION

Air quality is deteriorating with rapid industrial development and increases in the number of vehicles in East Asia (Deng *et al.*, 2012). Although emissions of SO_2 and NO_x in China have tended to decrease since 2006 and 2011, respectively (Xia *et al.*, 2016), the Chinese emissions are still 10–30 times those in Japan as reported by the Ministry of Environment of Japan (<http://www.env.go.jp/earth/ondanka/ghg/index03.html>). Atmospheric pollutants are transported across borders and influence neighboring

countries. For example, observations on islands such as Oki in Japan (Mukai *et al.*, 1990) and Jeju in Korea (Toppinga *et al.*, 2004), have characterized aerosols transported from continental East Asia.

In addition, Asian dust is a seasonal meteorological phenomenon in East Asia. Air masses including Asian dust export air pollutants emitted in the highly industrialized coastal areas of China (Uno *et al.*, 2003; Itahashi *et al.*, 2010; Hatakeyama *et al.*, 2014). The influence of Asian dust and anthropogenic air pollutants is of concern in Western Japan, particularly in Kyushu.

Recently, Uno *et al.* (2016) estimated that transboundary aerosols contribute 51% of the ammonium and 88% of the sulfate in aerosols in the Kyushu region. Although they performed a sensitivity analysis on a chemical transport model, their model could not reproduce the concentrations of nitrate in $\text{PM}_{2.5}$ and could not estimate the contribution

* Corresponding author.

Tel.: +81-480-73-8331; Fax: +81-480-70-2031
E-mail address: hatashir@cc.tuat.ac.jp

of transboundary nitrate in PM_{2.5}. In urban areas, nitrate (“fine nitrate”) occurs as fine particles of NH₄NO₃ (Tao *et al.*, 2014). Nitrate in coarse particles (“coarse nitrate”) results from the adsorption of HNO₃, produced by the dissociation of NH₄NO₃, onto the surface of dust or sea salt particles (Zhuang *et al.*, 1999; Takiguchi *et al.*, 2008). Sudheer and Rengarajan (2015) used a thermodynamic equilibrium model, ISORROPIA II, to calculate the diurnal variation of NH₃ and HNO₃: they reported that NH₃ and NH₄⁺ were in equilibrium with measured particulate and gas compositions. They also reported that HNO₃ deviated from thermodynamic equilibrium, possibly due to the uptake of HNO₃ gas on the surface of dust particles. Thermodynamic equilibrium models have difficulty in reproducing the transformation of fine nitrate to coarse nitrate.

To improve the reliability of model predictions, we investigated the size-segregated nitrate contribution in transboundary air pollution. To evaluate nitrate concentrations in transboundary air pollutants in Kumamoto, Japan, we distinguished the days dominated by transboundary air pollution from East Asia and the days dominated by local air pollution using a threshold of Pb concentration and the ratio Pb (in 0.5 < Dp < 1.0 μm)/Cu (in 2.5 < Dp < 10 μm).

Pb in fine particles is recognized as a useful tracer of transboundary air pollution. Pb is mainly derived from coal combustion. Sakata *et al.* (2014) reported that the concentration of Pb is strongly related to its emissions in the regions over which the air mass passed, particularly in the 30–40°N region of China, which is one of the highest emission areas in China. The annual consumption of coal in China amounted to 50% of total worldwide coal consumption in 2015 (BP Statistical Review of World Energy, 2016).

Cu is useful to identify vehicle-related emissions in Kumamoto (Taniguchi *et al.*, 2017). Cu in coarse particles is derived from tire wear (Hulskotte *et al.*, 2014), and is used as a tracer of local air pollution. Wilson and Suh (1997) reported that the half-life of coarse particles in the 1 < Dp < 10 μm size range is several minutes to several hours because coarse particles are easily removed by deposition. Therefore, when the contribution of transboundary air pollution is large, the Pb/Cu ratio is large.

The objectives of this study were (1) to develop an index that uses Pb concentration and the Pb/Cu ratio to distinguish between transboundary and local air pollution; (2) to investigate the effect of transboundary transport of nitrate in Kumamoto and Cape Hedo, Okinawa when long range transport occurred; and (3) to evaluate the size-segregated contribution of transboundary nitrate in Kumamoto.

EXPERIMENTAL METHODS

We observed the size distribution of mass concentration, ionic composition and content of trace metals in aerosols. Size-segregated sampling of aerosols was carried out at a site in Kumamoto City (hereafter referred to as KM) in October and December of 2014; March, July to August, and October of 2015; and March of 2016. Sampling was also conducted at a rural site at Cape Hedo (hereafter referred to as HD) in April, October, and December of 2012; April,

October, and December of 2013; April and October of 2014; and March and October to November of 2015. All the sampling periods are listed in Table 1.

The locations of KM and HD are shown in Fig. 1. Since HD is usually closed in summer because of frequent attacks of typhoon, summer data at HD was not available. KM (32.81°N, 130.73°E; 30 m above sea level) is located in southwestern Japan on the major island of Kyushu, about 1350 km from Beijing and about 700 km from HD. Air masses arrive from the continent earlier at KM than at HD. The population of Kumamoto City is 740,000 and KM is an urban site with heavy traffic. HD (26.87°N, 128.25°E; 60 m above sea level) is located at the northern end of Okinawa Island, about 100 km from Naha, the largest city on the island, and about 650 km from Shanghai, China. There are no large industrial or residential areas near HD. Air masses reaching HD are transported from China, Korea, Japan, Southeast Asia, or the Pacific Ocean, depending on prevailing wind patterns; so, this site is suitably located to observe the long-range transport of air pollutants from East Asia.

Samples were collected in a six-stage cascade impactor (Nanosampler Model 3180, Kanomax, Osaka, Japan). Ambient air was sampled with a diaphragm vacuum pump (DA-121D, Ulvac, Kanagawa, Japan) with a mass flow controller (Model 8550, Kofloc, Kyoto, Japan) set at 40 L min⁻¹. For every experiment, sampling duration was 24 hours. Aerosols of Dp > 10 μm, 10 > Dp > 2.5 μm, 2.5 > Dp > 1 μm, 1 > Dp > 0.5 μm, 0.5 > Dp > 0.1 μm, and Dp < 0.1 μm were collected on PTFE filters of 55 mm diameter (PF020, Advantec, Tokyo, Japan) on the respective stages of the sampler. After sampling, filters were cut into two pieces; one piece was used for analyses of ionic components and the other for trace metals. The filters were weighed on an ultra-micro balance (UMX2, Mettler Toledo International, Ohaio, USA) before and after sampling to obtain the total mass in each size range.

Meteorological data at the sites were obtained for nearby

Table 1. Sampling periods.

| | year | season | month | day |
|----|------|--------|-----------|----------------|
| HD | 2012 | Spring | Apr. | 22–28 |
| | | Autumn | Oct. | 11–16 |
| | | Winter | Dec. | 11–16 |
| | 2013 | Spring | Apr. | 24–30 |
| | | Autumn | Oct. | 13–18 |
| | | Winter | Dec. | 13–17 |
| | 2014 | Spring | Apr. | 13–17 |
| | | Autumn | Oct. | 17–21 |
| | 2015 | Spring | Mar. | 12–17 |
| | | Autumn | Oct.–Nov. | Oct. 26–Nov. 7 |
| | 2016 | Spring | Mar. | 1–7 |
| | | Autumn | Oct. | 14–21 |
| KM | 2014 | Autumn | Oct. | 14–21 |
| | | Winter | Dec. | 17–21 |
| | | Spring | Mar. | 12–17 |
| | 2015 | Summer | Jul.–Aug. | Jul. 27–Aug. 2 |
| | | Autumn | Oct. | 26–31 |
| | 2016 | Spring | Mar. | 1–7 |

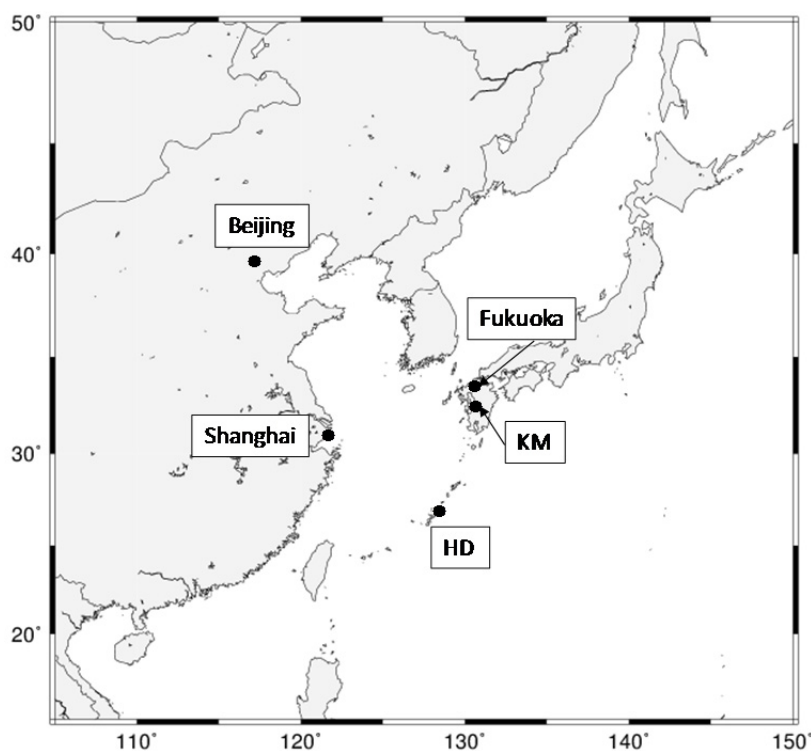


Fig. 1. The location of KM, HD, Fukuoka city, Beijing and Shanghai.

weather stations through the Japan Meteorological Agency website (<http://www.data.jma.go.jp/obd/stats/etrn/index.php>). To identify the transport pathways of air masses, backward trajectories starting from KM and HD at a height of 500 m above sea level were calculated on the NOAA website <http://ready.arl.noaa.gov/hypub-bin/trajtype.pl> with the HYbrid Single-Particle Lagrangian Integrated Trajectory model (HYSPLIT).

Ionic species in size-segregated aerosols were quantitatively analyzed after ultrasonic extraction for 20 min in a mixture of ethanol (100 μL) and distilled water (10 mL) in a polypropylene tube. Cl^- , NO_3^- , SO_4^{2-} , Na^+ , NH_4^+ , K^+ , Mg^{2+} , and Ca^{2+} were analyzed by ion chromatography (LC10AD, Shimadzu, Kyoto, Japan). Anions were separated by a column for anions (IC-SA2, Shimadzu, Kyoto, Japan) and detected by a conductivity detector (CDD-10ASP, Shimadzu, Kyoto, Japan) with a suppresser. Cations were separated by a column for cations (IC-C4, Shimadzu, Kyoto, Japan) and detected by a conductivity detector (CDD-6A, Shimadzu, Kyoto, Japan) without a suppresser. Concentrations of metallic elements were measured and analyzed by Taniguchi *et al.* (2017). Concentration of each ionic component (detection limit of each ion is $0.01 \mu\text{g m}^{-3}$) and element was calculated by subtracting blank value (Hatakeyama *et al.*, 2011; Yumoto *et al.* 2015). Each chemical component showed satisfactory recovery in the range of 90–107%.

RESULTS AND DISCUSSION

Characteristics of Ionic Components

Table 2 shows the size-segregated concentrations of ionic components of particles and the fraction of each ion at KM

in spring, summer, autumn, and winter. Ionic composition did not differ among seasons except for nitrate in summer. In spring, autumn, and winter, ammonium, nitrate, and sulfate were the major components in particles in the $D_p < 2.5 \mu\text{m}$ size-range: the percentages of ammonium, nitrate, and sulfate were approximately 25%, 20%, and 55% in particles in the $D_p < 2.5 \mu\text{m}$ size-range in spring, autumn, and winter, respectively. In contrast, in summer, ammonium and sulfate were the major components in the $D_p < 2.5\text{-}\mu\text{m}$ particles: the percentages of ammonium and sulfate were approximately 25% and 70%, respectively. In $D_p > 2.5\text{-}\mu\text{m}$ particles, sodium, calcium, chloride and nitrate were major components in every season.

The ionic composition at HD was different from that at KM. Table 3 shows the size-segregated concentrations (and percentages) of ionic components of particles at HD in spring, autumn, and winter (samples were not taken during summer): the ionic composition did not differ among these seasons. Ammonium and sulfate were the dominant components in particles smaller than $2.5 \mu\text{m}$: the percentages of ammonium and sulfate were approximately 20% and 75%, respectively. In $D_p > 2.5\text{-}\mu\text{m}$ particles, sodium and chloride were the dominant components in every season sampled.

The size-segregated concentrations of Pb and Cu at KM in spring, summer, autumn, and winter are listed in Table S1 and those at HD in spring, autumn, and winter are listed in Table S2.

An Index to Classify Transboundary and Local Air Pollution at KM

At KM, we distinguished days influenced mainly by long-range transport from days influenced mainly by local

Table 2. Size-segregated concentration of ionic components and the fraction of each ion at KM in spring, summer, autumn, and winter.

| Dp (μm) | Na^+ | | NH_4^+ | | K^+ | | Mg^{2+} | | Ca^{2+} | | Cl^- | | NO_3^- | | SO_4^{2-} | |
|----------------------|----------------------|----|----------------------|----|----------------------|---|----------------------|---|----------------------|----|----------------------|----|----------------------|----|----------------------|----|
| | $\mu\text{g m}^{-3}$ | % | $\mu\text{g m}^{-3}$ | % | $\mu\text{g m}^{-3}$ | % | $\mu\text{g m}^{-3}$ | % | $\mu\text{g m}^{-3}$ | % | $\mu\text{g m}^{-3}$ | % | $\mu\text{g m}^{-3}$ | % | $\mu\text{g m}^{-3}$ | % |
| spring | | | | | | | | | | | | | | | | |
| –0.1 | 0.00 | 0 | 0.22 | 25 | 0.03 | 3 | 0.00 | 0 | 0.02 | 2 | 0.01 | 1 | 0.11 | 12 | 0.52 | 57 |
| 0.1–0.5 | 0.02 | 0 | 0.97 | 26 | 0.09 | 2 | 0.00 | 0 | 0.00 | 0 | 0.04 | 1 | 0.6 | 16 | 2.06 | 55 |
| 0.5–1 | 0.02 | 0 | 1.58 | 26 | 0.06 | 1 | 0.00 | 0 | 0.02 | 0 | 0.1 | 2 | 1.39 | 23 | 2.88 | 48 |
| 1–2.5 | 0.08 | 2 | 0.70 | 20 | 0.04 | 1 | 0.02 | 1 | 0.11 | 3 | 0.08 | 2 | 1.08 | 32 | 1.32 | 39 |
| 2.5–10 | 0.15 | 8 | 0.09 | 5 | 0.02 | 1 | 0.03 | 2 | 0.24 | 13 | 0.1 | 6 | 0.93 | 50 | 0.3 | 16 |
| 10– | 0.03 | 9 | 0.02 | 6 | 0.00 | 0 | 0.00 | 1 | 0.06 | 20 | 0.03 | 9 | 0.09 | 30 | 0.07 | 24 |
| summer | | | | | | | | | | | | | | | | |
| –0.1 | 0.00 | 2 | 0.07 | 22 | 0.01 | 3 | 0.00 | 0 | 0.00 | 1 | 0.00 | 1 | 0.01 | 5 | 0.2 | 67 |
| 0.1–0.5 | 0.02 | 1 | 0.56 | 25 | 0.05 | 2 | 0.00 | 0 | 0.00 | 0 | 0.00 | 0 | 0 | 0 | 1.65 | 72 |
| 0.5–1 | 0.04 | 1 | 1.41 | 26 | 0.08 | 2 | 0.00 | 0 | 0.00 | 0 | 0.00 | 0 | 0.01 | 0 | 3.95 | 72 |
| 1–2.5 | 0.40 | 16 | 0.21 | 9 | 0.05 | 2 | 0.04 | 2 | 0.04 | 1 | 0.13 | 5 | 0.64 | 26 | 0.95 | 39 |
| 2.5–10 | 0.74 | 22 | 0.04 | 1 | 0.05 | 1 | 0.08 | 2 | 0.09 | 3 | 0.42 | 13 | 1.5 | 45 | 0.4 | 12 |
| 10– | 0.06 | 19 | 0.01 | 2 | 0.00 | 1 | 0.01 | 2 | 0.02 | 8 | 0.05 | 16 | 0.11 | 36 | 0.05 | 16 |
| autumn | | | | | | | | | | | | | | | | |
| –0.1 | 0.01 | 1 | 0.12 | 18 | 0.04 | 6 | 0.00 | 0 | 0.02 | 3 | 0.01 | 1 | 0.05 | 7 | 0.43 | 64 |
| 0.1–0.5 | 0.02 | 1 | 0.55 | 21 | 0.15 | 6 | 0.00 | 0 | 0.00 | 0 | 0.03 | 1 | 0.28 | 11 | 1.6 | 61 |
| 0.5–1 | 0.03 | 1 | 0.72 | 22 | 0.13 | 4 | 0.00 | 0 | 0.02 | 1 | 0.05 | 1 | 0.35 | 11 | 1.91 | 60 |
| 1–2.5 | 0.14 | 10 | 0.15 | 10 | 0.04 | 3 | 0.02 | 1 | 0.06 | 4 | 0.10 | 7 | 0.47 | 31 | 0.51 | 34 |
| 2.5–10 | 0.43 | 17 | 0.04 | 2 | 0.05 | 2 | 0.06 | 2 | 0.19 | 8 | 0.40 | 16 | 1.10 | 44 | 0.24 | 10 |
| 10– | 0.12 | 21 | 0.01 | 1 | 0.01 | 1 | 0.01 | 2 | 0.06 | 10 | 0.16 | 28 | 0.14 | 25 | 0.06 | 11 |
| winter | | | | | | | | | | | | | | | | |
| –0.1 | 0.01 | 2 | 0.12 | 25 | 0.00 | 1 | 0.00 | 0 | 0.00 | 1 | 0.03 | 6 | 0.07 | 15 | 0.23 | 50 |
| 0.1–0.5 | 0.01 | 1 | 0.51 | 25 | 0.06 | 3 | 0.00 | 0 | 0.00 | 0 | 0.07 | 4 | 0.40 | 19 | 1.02 | 49 |
| 0.5–1 | 0.03 | 1 | 0.73 | 25 | 0.05 | 2 | 0.00 | 0 | 0.01 | 0 | 0.12 | 4 | 0.63 | 22 | 1.33 | 46 |
| 1–2.5 | 0.12 | 8 | 0.25 | 17 | 0.04 | 3 | 0.01 | 1 | 0.03 | 2 | 0.11 | 8 | 0.50 | 33 | 0.44 | 29 |
| 2.5–10 | 0.35 | 22 | 0.05 | 3 | 0.02 | 1 | 0.04 | 2 | 0.09 | 6 | 0.38 | 24 | 0.46 | 30 | 0.18 | 12 |
| 10– | 0.19 | 31 | 0.00 | 0 | 0.01 | 1 | 0.02 | 3 | 0.02 | 4 | 0.24 | 39 | 0.06 | 10 | 0.07 | 12 |

air pollution by Pb concentrations and Pb/Cu ratios. We defined conditions in which the Pb concentration was higher than 10 ng m^{-3} and the Pb/Cu ratio was larger than 1.75 as being dominated by long-range transport. The threshold Pb concentration of 10 ng m^{-3} is the average concentration at Fukue Island, in the East China Sea just west of Kyushu, in spring and winter when long-range transport is dominant (Suzuki *et al.*, 2014). Frequently in spring and winter, the air at HD, Fukue Island, and Fukuoka city is dominated by air masses transported from East Asia (Suzuki *et al.*, 2014; Shimada *et al.*, 2015). Sometimes such air masses pass over large cities in Kyushu such as Kumamoto and Fukuoka before arriving at HD (Taniguchi *et al.*, 2017).

We defined conditions in which the Pb/Cu ratio was lower than 1.75 and the Pb concentration was lower than 5.00 ng m^{-3} as being dominated by local air pollution. The Pb concentration of 5.00 ng m^{-3} was the median value at KM during our campaign. Thus, when the Pb concentration was larger than 5.00 ng m^{-3} , the source of the aerosols was regarded as a mixture of long-range transport and local air pollution.

Cu in coarse particles can be used as a tracer of aerosols produced by local vehicles in KM (Taniguchi *et al.*, 2017). We can analyze Pb/Cu ratio when the air mass passing over Fukuoka, which is north of Kumamoto, has been transported

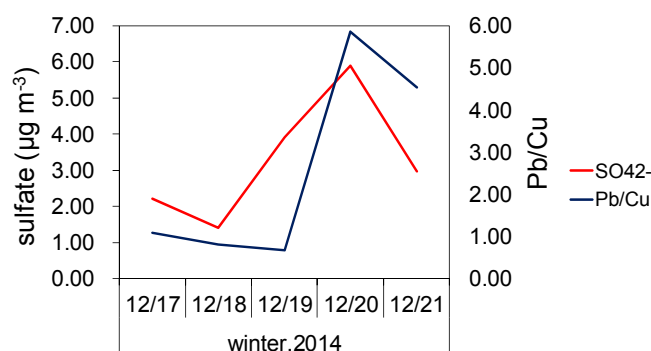
from East Asia. One example is as follows. On 20 Dec. 2014, the sulfate aerosols in KM were found to have been transported from East Asia based on simulation results from the CFORS model (<http://www-cfors.nies.go.jp/~cfors/index.html>). Sulfate is a useful tracer to identify pollution in the Kyushu region that has been transported long distances (Kaneyasu *et al.*, 2014). On 20 Dec., when sulfate transported from East Asia arrived at KM, sulfate concentrations and Pb/Cu ratios were significantly higher than on other days (Fig. 2). Hence, we could distinguish between local air pollution and long-range transport based on Pb/Cu ratios and Pb concentration.

Size Distribution of Nitrate under Long-Range Transport and Local Air Pollution Conditions at KM and HD

For HD, we distinguished long-range transport by backward trajectories and Pb concentrations. If an air mass had passed over the Asian continent within 72 hours before it reached HD and the concentration of Pb was higher than 5.00 ng m^{-3} , then we classified it as long-range transport. The average Pb concentration at HD was 5.00 ng m^{-3} during our sampling days. Because the concentration of Cu at HD was often below the detection limit, we did not base our recognition of long-range transport conditions on the Pb/Cu ratio.

Table 3. Size-segregated concentration of ionic components and the fraction of each ion at HD in spring, autumn, and winter.

| Dp (μm) | Na^+ | | NH_4^+ | | K^+ | | Mg^{2+} | | Ca^{2+} | | Cl^- | | NO_3^- | | SO_4^{2-} | |
|----------------------|----------------------|----|----------------------|----|----------------------|---|----------------------|---|----------------------|---|----------------------|----|----------------------|----|----------------------|----|
| | $\mu\text{g m}^{-3}$ | % | $\mu\text{g m}^{-3}$ | % | $\mu\text{g m}^{-3}$ | % | $\mu\text{g m}^{-3}$ | % | $\mu\text{g m}^{-3}$ | % | $\mu\text{g m}^{-3}$ | % | $\mu\text{g m}^{-3}$ | % | $\mu\text{g m}^{-3}$ | % |
| spring | | | | | | | | | | | | | | | | |
| –0.1 | 0.00 | 1 | 0.04 | 19 | 0.01 | 4 | 0.00 | 1 | 0.00 | 1 | 0.00 | 2 | 0.01 | 3 | 0.13 | 69 |
| 0.1–0.5 | 0.00 | 0 | 0.21 | 24 | 0.01 | 2 | 0.00 | 0 | 0.00 | 0 | 0.00 | 0 | 0.00 | 1 | 0.64 | 73 |
| 0.5–1 | 0.02 | 1 | 0.47 | 23 | 0.04 | 2 | 0.01 | 0 | 0.01 | 0 | 0.01 | 0 | 0.01 | 0 | 1.45 | 72 |
| 1–2.5 | 0.37 | 14 | 0.31 | 11 | 0.06 | 2 | 0.06 | 2 | 0.05 | 2 | 0.33 | 12 | 0.26 | 10 | 1.31 | 48 |
| 2.5–10 | 1.89 | 27 | 0.01 | 0 | 0.14 | 2 | 0.23 | 3 | 0.20 | 3 | 2.78 | 40 | 1.06 | 15 | 0.70 | 10 |
| 10– | 0.76 | 30 | 0.00 | 0 | 0.04 | 2 | 0.09 | 3 | 0.06 | 2 | 1.24 | 48 | 0.15 | 6 | 0.23 | 9 |
| autumn | | | | | | | | | | | | | | | | |
| –0.1 | 0.01 | 4 | 0.02 | 16 | 0.00 | 1 | 0.00 | 0 | 0.00 | 2 | 0.01 | 4 | 0.00 | 0 | 0.11 | 73 |
| 0.1–0.5 | 0.01 | 1 | 0.21 | 19 | 0.02 | 1 | 0.00 | 0 | 0.00 | 0 | 0.00 | 0 | 0.00 | 0 | 0.85 | 77 |
| 0.5–1 | 0.04 | 2 | 0.36 | 19 | 0.04 | 2 | 0.01 | 0 | 0.00 | 0 | 0.01 | 0 | 0.00 | 0 | 1.49 | 77 |
| 1–2.5 | 0.77 | 24 | 0.12 | 4 | 0.05 | 2 | 0.09 | 3 | 0.05 | 2 | 0.93 | 30 | 0.33 | 10 | 0.82 | 26 |
| 2.5–10 | 3.10 | 29 | 0.06 | 1 | 0.14 | 1 | 0.36 | 3 | 0.19 | 2 | 4.99 | 46 | 1.04 | 10 | 0.91 | 8 |
| 10– | 1.45 | 30 | 0.02 | 0 | 0.06 | 1 | 0.15 | 3 | 0.07 | 1 | 2.46 | 51 | 0.20 | 4 | 0.38 | 8 |
| winter | | | | | | | | | | | | | | | | |
| –0.1 | 0.00 | 3 | 0.02 | 18 | 0.00 | 3 | 0.00 | 0 | 0.00 | 1 | 0.00 | 2 | 0.00 | 2 | 0.09 | 71 |
| 0.1–0.5 | 0.00 | 0 | 0.21 | 19 | 0.01 | 1 | 0.00 | 0 | 0.00 | 0 | 0.00 | 0 | 0.00 | 0 | 0.89 | 80 |
| 0.5–1 | 0.01 | 1 | 0.32 | 17 | 0.01 | 1 | 0.01 | 0 | 0.00 | 0 | 0.00 | 0 | 0.01 | 0 | 1.50 | 81 |
| 1–2.5 | 0.32 | 17 | 0.15 | 8 | 0.03 | 2 | 0.05 | 3 | 0.03 | 2 | 0.33 | 17 | 0.20 | 10 | 0.83 | 43 |
| 2.5–10 | 1.63 | 29 | 0.05 | 1 | 0.08 | 1 | 0.19 | 3 | 0.11 | 2 | 2.34 | 41 | 0.77 | 13 | 0.52 | 9 |
| 10– | 0.78 | 31 | 0.02 | 1 | 0.01 | 1 | 0.09 | 4 | 0.04 | 2 | 1.17 | 47 | 0.15 | 6 | 0.24 | 10 |

**Fig. 2.** Total sulfate concentration in all particle size ranges and Pb/Cu ratio during the Dec. 2014 campaign at KM.

At HD under long-range transport conditions, nitrate in particles in the $2.5 < D_p < 10 \mu\text{m}$ size range was distributed unimodally (Fig. 3); the concentration of nitrate in $2.5 < D_p < 10 \mu\text{m}$ particles was $1.83 \mu\text{g m}^{-3}$. The concentrations of nitrate in $D_p < 0.1 \mu\text{m}$, $0.1 < D_p < 0.5 \mu\text{m}$ and $0.5 < D_p < 1 \mu\text{m}$ particles were very low (total $< 0.1 \mu\text{g m}^{-3}$); thus, fine nitrate was not transported from the continent during long-range transport.

Tagiguchi *et al.* (2008) reported the relation between the transport time and size distribution of nitrate. The fraction of nitrate of $\text{PM}_{1.1}$ ($= \text{PM}_{1.1} \text{NO}_3^-$) among all particle sizes ($t\text{NO}_3^-$) was 0.5–0.9 at Qingdao, China, while that at HD was below 0.1 when the transport time of the air mass from Qingdao to HD was over 48 hours. This observation implies that during long-range transport, nitrate in fine particles shifted to coarse particles.

To quantify the impact of locally emitted pollutants from the Kyushu region on the atmospheric environment at HD,

we compared the concentrations of nitrate at HD and KM in an air mass that passed over KM and reached HD on the same day. For example, air masses arriving at HD from 10:00 Oct. 17 to 10:00 Oct. 18 passed over Kumamoto or its vicinity before arriving at HD as shown in Fig. 4. The transport time from KM to HD on 17 Oct. 2014 is estimated to be about 24 hours based on the backward trajectory calculations (Fig. 4); therefore, the air mass at KM on 16 Oct. 2014 reached HD on 17 Oct. 2014. Table 4 shows the concentrations of nitrate on 16 and 17 Oct. 2014 at KM and HD, respectively.

The size distribution of nitrate at both KM and HD did not greatly differ for particles larger than $1 \mu\text{m}$ (Fig. 3). About 35% of nitrate at KM existed in particles with $D_p < 1 \mu\text{m}$; in contrast, less than 1% of nitrate at HD existed in particles with $D_p < 1 \mu\text{m}$. Therefore, we conclude that fine nitrate emitted from the Kyushu region did not reach HD even when air masses passed over KM and reached HD.

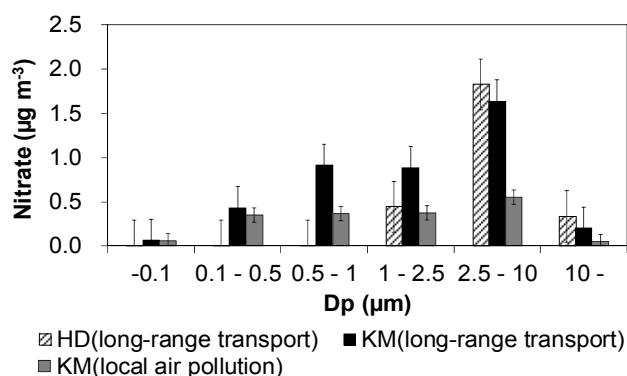


Fig. 3. Size distribution of nitrate in particles at KM and HD under long-range transport (long-range transport) and local air pollution (local air pollution) conditions.

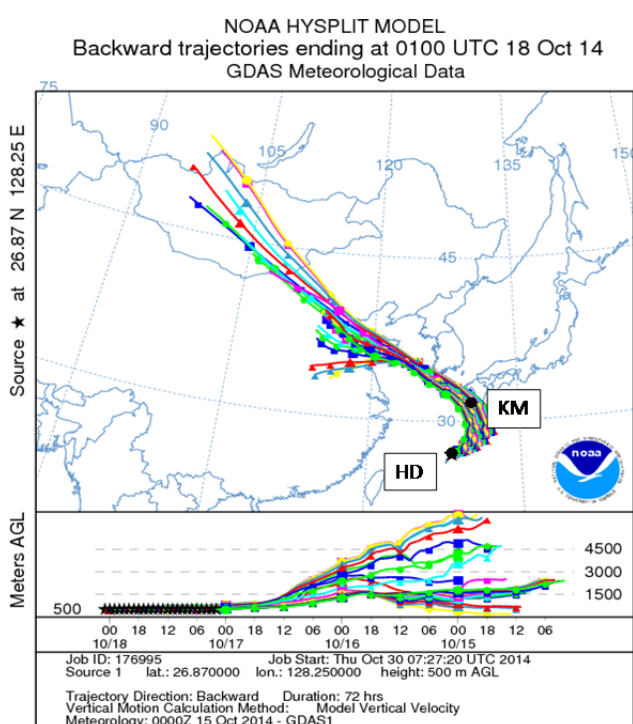


Fig. 4. Backward trajectories arriving at HD at every hour on the hour from 10:00 JST (01:00 UTC) on Oct. 17 to 10:00 Oct. 18, 2014.

Table 4. Concentrations of nitrate ($\mu\text{g m}^{-3}$) at KM on 16 Oct. 2014 and at HD on 17 Oct. 2014.

| Dp (μm) | KM | HD |
|----------------------|------|------|
| -0.1 | 0.05 | nd |
| 0.1–0.5 | 0.42 | 0.01 |
| 0.5–1 | 1.09 | nd |
| 1–2.5 | 0.78 | 0.49 |
| 2.5–10 | 1.82 | 2.33 |
| 10– | 0.34 | 0.57 |

Also, the high temperature at HD on 17 Oct. 2014 (23.1°C) must have caused the decomposition of NH_4NO_3 , and as a result fine nitrate was not observed there. The major

components in $\text{PM}_{2.5}$ at HD were sulfate and ammonium. Furthermore, the concentration of coarse nitrate ($D_p > 1 \mu\text{m}$) at HD on 17 Oct. was higher than at KM on 16 Oct. The concentration of nitrate in the particles of $2.5 < D_p < 10 \mu\text{m}$ at HD ($2.33 \mu\text{g m}^{-3}$) was about 1.3 times that at KM ($1.83 \mu\text{g m}^{-3}$). The concentration of coarse nitrate in the air mass at HD increased because of the dissociation and adsorption of fine nitrate. At HD, the impact of nitrate emitted from the continent and the Kyushu region could be found only in particles of $D_p > 1 \mu\text{m}$.

Effect of Emissions from a Nearby Megacity

At KM, the air mass under local air pollution conditions usually contains air transported by northerly winds. Therefore, local pollution from Kumamoto is augmented by pollution emitted from Fukuoka, a city of 1.5 million approximately 100 km north of Kumamoto. In cases of long-range transport at KM, the prevailing northerly winds can carry emissions from both China and Fukuoka. When the contribution of nitrate in long-range transport is estimated, the pollution emitted in Fukuoka should be subtracted to estimate pollution originating from the continent.

Nitrate concentration in the size range $0.5 < D_p < 1 \mu\text{m}$ was $0.92 \mu\text{g m}^{-3}$ (Fig. 3). The peak concentration was found in the $2.5 < D_p < 10 \mu\text{m}$ range ($1.64 \mu\text{g m}^{-3}$). In contrast, nitrate concentrations under local air pollution conditions were lower (Fig. 3), and the concentration of every particle size class between 0.1 and $10 \mu\text{m}$ was $0.35\text{--}0.55 \mu\text{g m}^{-3}$. The total concentration of nitrate in particles of all sizes under local air pollution conditions was $1.75 \mu\text{g m}^{-3}$, which is less than half that under long-range transport conditions. The concentrations of nitrate in the particle size ranges of $0.5 < D_p < 1 \mu\text{m}$ and $2.5 < D_p < 10 \mu\text{m}$ under long-range transport conditions were approximately 2.5 and 3 times as high as those under local air pollution conditions, respectively. Therefore, we conclude that the nitrate in both fine and coarse particles was transported from long distances away.

Fig. 5 show size distributions and size-segregated concentrations of nitrate at KM in spring, autumn, and winter. The average temperature at KM was 9.8, 16.8, and 7.7°C in spring, autumn and winter, respectively. In winter, nitrate concentrations under local air pollution conditions were highest in particles in the $0.1 < D_p < 0.5 \mu\text{m}$ size range. Low temperature conditions facilitate formation of fine nitrate (NH_4NO_3 particles) (Seinfeld and Pandis, 2006). In urban areas of Shanghai NH_4NO_3 concentrations were reported to be highest in the $0.3 < D_p < 0.5 \mu\text{m}$ size range (Zhao and Gao, 2007). In contrast, in spring and autumn, nitrate concentrations under local air pollution conditions were highest in the $2.5 < D_p < 10 \mu\text{m}$ range. The distribution of nitrate in autumn was unimodal with the peak in the $2.5 < D_p < 10 \mu\text{m}$ range under both local air pollution and long-range transport conditions. Nitrate in the $0.5 < D_p < 10 \mu\text{m}$ size ranges in spring under long-range transport conditions shows higher concentration among all particle sizes. Nitrate concentrations in winter under long-range transport conditions were similar in the $0.5 < D_p < 1 \mu\text{m}$, $1 < D_p < 2.5 \mu\text{m}$, and $2.5 < D_p < 10 \mu\text{m}$ size ranges: 1.48, 1.40, $1.68 \mu\text{g m}^{-3}$, respectively. Thus, we conclude that

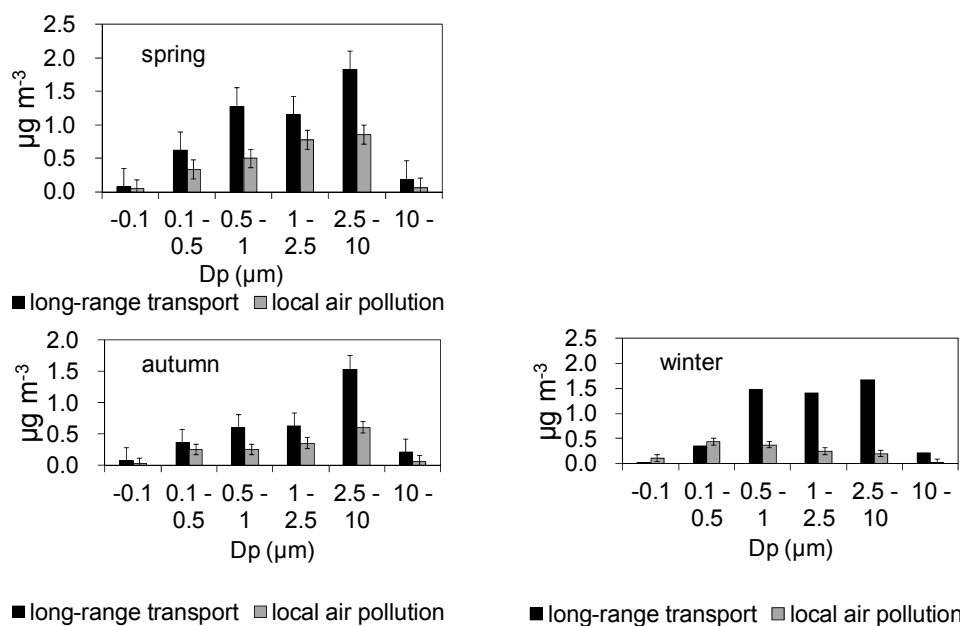


Fig. 5. Size distribution of nitrate in particles at KM under long-range transport (long-range transport) and local air pollution (local air pollution) conditions in spring, autumn, and winter.

even under local air pollution conditions, conversion of fine nitrate to coarse nitrate can occur in warmer seasons.

Contribution of Transboundary Nitrate at KM

In order to estimate the contribution of transboundary nitrate at KM, the concentrations of nitrate under long-range transport and local air pollution conditions were considered separately. In this study we calculated the contribution of long-range transport by the following equation.

$$\text{Contribution of transport} = \frac{\{(\text{conc. at transport event}) - (\text{conc. at local only event})\}}{(\text{conc. at transport event})} \quad (1)$$

The concentrations of transboundary nitrate in whole seasons at KM were 0.05, 0.10, 0.49, 0.17, 1.00, and 0.21 $\mu\text{g m}^{-3}$ in particles in the evaluated size ranges $D_p < 0.1$; 0.1–0.5; 0.5–1; 1–2.5; 2.5–10; and $> 10 \mu\text{m}$, respectively. The contribution of trans-boundary nitrate (%) at KM in spring, autumn, winter and whole seasons is shown in Table 5. Of the total transboundary nitrate, 40% and 60% existed in the $D_p < 2.5 \mu\text{m}$ and $> 2.5 \mu\text{m}$ particles, respectively.

Coarse particles contained more nitrate transported from China than did fine particles. However, transboundary nitrate in fine particles was not negligible. The contribution of transboundary nitrate in fine particles to the total transboundary nitrate in whole seasons at KM was largest in particles in the $0.5 < D_p < 1 \mu\text{m}$ range at approximately 60%. In contrast, the contribution in particles in the $0.1 < D_p < 0.5 \mu\text{m}$ size range was approximately 20%. Although the nitrate in Kumamoto and Fukuoka was predominantly in particles in the $0.1 < D_p < 0.5 \mu\text{m}$ size range, the contributions of transboundary nitrate in particles in the $0.5 < D_p < 1 \mu\text{m}$ and $1 < D_p < 2.5 \mu\text{m}$ size ranges to the total nitrate in those size ranges were approximately 60%, and the contribution in the $2.5 < D_p < 10 \mu\text{m}$ size range was approximately 65%.

Table 5. The contribution of trans-boundary nitrate (%) at KM in spring, autumn, winter, and whole seasons.

| D_p (μm) | spring | autumn | winter | whole seasons |
|-------------------------|--------|--------|--------|---------------|
| –0.1 | 41 | 57 | nd | 5 |
| 0.1–0.5 | 46 | 29 | nd | 20 |
| 0.5–1 | 61 | 57 | 75 | 60 |
| 1–2.5 | 33 | 43 | 83 | 58 |
| 2.5–10 | 53 | 60 | 88 | 66 |
| 10– | 63 | 70 | 91 | 74 |

In spring, autumn, and winter, the contribution of transboundary nitrate in particles smaller than $2.5 \mu\text{m}$ to nitrate in particles smaller than $2.5 \mu\text{m}$ was approximately 50%, 50%, and 70%, respectively. Under higher temperatures in autumn (average 16.8°C), transboundary nitrate in particles smaller than $2.5 \mu\text{m}$ was not transported as far as in spring and winter (9.8 and 7.7°C , respectively). The contribution of transboundary nitrate in all particle sizes to total nitrate was approximately 50%, 50% and 60% in spring, autumn and winter, respectively.

The contribution of transboundary nitrate in all particle sizes to total nitrate was about 58% in whole seasons at KM. Prospero and Savoie (1989) measured the concentration of nitrate in the North Pacific Ocean that had been transported from the Asian continent with Asian dust and estimated that the contribution of anthropogenic nitrate was about 40–70%; our results are in agreement.

Uno et al. (2016) estimated that the contribution of transboundary nitrate in total suspended particles was approximately 70% when Asian dust was transported to the northern Kyushu region in May, 2015; our results are in fair agreement with this estimate.

In summary, we found that transboundary nitrate was found largely in particles from 0.5 to $10 \mu\text{m}$, and that the

contribution of transboundary nitrate in the particle size range of 0.1 to 0.5 μm was about 20% even under long-range transport conditions.

CONCLUSIONS

Fine nitrate scarcely reached HD from the Asian continent under long-range transport conditions. Neither was fine nitrate emitted in the Kyushu region transported to HD, even in a case when the air mass passed over KM one day before arriving at HD. The contribution of transboundary nitrate in the $0.5 < D_p < 10 \mu\text{m}$ particle size range in whole seasons at KM was substantial and the contribution of transboundary nitrate in the particle size range of $0.1 < D_p < 0.5 \mu\text{m}$ was about 20% even under long-range transport conditions. The contribution of transboundary nitrate in particles in the $D_p < 2.5 \mu\text{m}$ size range at KM was approximately 50%, 50%, and 70% in spring, autumn and winter, respectively.

ACKNOWLEDGEMENTS

This research was supported by the Global Environmental Research Fund (5-1452 and 2-1403) of the Ministry of the Environment of Japan.

SUPPLEMENTARY MATERIAL

Supplementary data associated with this article can be found in the online version at <http://www.aaqr.org>.

REFERENCES

- BP Statistical Review of the World Energy (2016). <http://www.bp.com/en/global/corporate/energy-economics/statistical-review-of-world-energy.html>
- Deng, J., Du, K., Wang, K., Yuan, C.S. and Zhao, J. (2012). Long-term atmospheric visibility trend in Southeast China, 1973–2010. *Atmos. Environ.* 59: 11–21.
- Hatakeyama, S., Hanaoka, S., Ikeda, K., Watanabe, I., Arakaki, T., Sadanaga, Y., Bandow, H., Kato, S., Kajii, Y., Sato, K., Shimizu, A. and Takami, A. (2011). Aerial observation of aerosols transported from East Asia chemical composition of aerosols and layered structure of an air mass over the East China Sea. *Aerosol Air Qual. Res.* 11: 497–507.
- Hatakeyama, S., Ikeda, K., Hanaoka, S., Watanabe, I., Arakaki, T., Bandow, H., Sadanaga, Y., Kato, S., Kajii, Y., Zhang, D., Okuyama, K., Ogi, T., Fujimoto, T., Seto, T., Shimizu, A., Sugimoto, N. and Takami, A. (2014). Aerial observations of air masses transported from East Asia to the Western Pacific: Vertical structure of polluted air masses. *Atmos. Environ.* 97: 456–461.
- Hulskotte, J.H.J., Roskam, G.D. and Denier van der Gon, H.A.C. (2014). Elemental composition of current automotive braking materials and derived air emission factors. *Atmos. Environ.* 99: 436–445.
- Itahashi, S., Yumimoto, K., Uno, I., Eguchi, K., Takemura, T., Hara, Y., Shimizu, A., Sugimoto, N. and Liu, Z. (2010). Structure of dust and air pollutant outflow over East Asia in the spring. *Geophys. Res. Lett.* 37: L20806.
- Kaneyasu, N., Yamamoto, S., Sato, K., Takami, A., Hayashi, M., Hara, K., Kawamoto, K., Okuda, T. and Hatakeyama, S. (2014). Impact of long-range transport of aerosols on the $\text{PM}_{2.5}$ concentration at a major metropolitan area in the northern Kyushu area of Japan. *Atmos. Environ.* 97: 416–425.
- Mukai, H., Ambe, Y., Shibata, K., Muku, T., Takeshita, K., Fukuma, T., Takahashi, J. and Mizota, S. (1990). Long-term variation of chemical composition of atmospheric aerosol on the Oki Islands in the Sea of Japan. *Atmos. Environ.* 24: 1379–1390.
- Prospero, J.M. and Savoie, D.L. (1989) Effect of continental sources on nitrate concentration over the Pacific Ocean. *Nature* 339: 687–689.
- Sakata, M., Ishikawa, T. and Mitsunobu, S. (2014). Contribution of Asian outflow to atmospheric concentrations of sulfate and trace elements in aerosols during winter in Japan. *Geochem. J.* 48: 479–490.
- Seinfeld, J.H. and Pandis, S.N. (2006). *Atmospheric chemistry and physics: From air pollution to climate change*, 2nd ed., John Wiley & Sons, New York, USA, pp. 470–485.
- Shimada, K., Shimada, M., Takami, A., Hasegawa, S., Fushimi, A., Arakaki, T., Watanabe, I. and Hatakeyama, S. (2015). Mode and place of origin of carbonaceous aerosols transported from East Asia to Cape Hedo, Okinawa, Japan. *Aerosol Air Qual. Res.* 15: 799–813.
- Sudheer, A.K. and Rengarajan, R. (2015). Time-resolved inorganic chemical composition of fine aerosol and associated precursor gases over an urban environment in western India: Gas-aerosol equilibrium characteristics. *Atmos. Environ.* 109: 217–227.
- Suzuki, R., Yoshino, A., Kaneyasu, N., Takami, A., Hayashi, M., Hara, K., Watanabe, I. and Hatakeyama, S. (2014). Characteristics and source apportionment of trace metals in the aerosols at Fukue and Fukuoka City. *J. Japan Soc. Atmos. Environ.* 49: 15–25 (in Japanese).
- Tagiguchi, Y., Takami, A., Sadanaga, Y., Lun, X., Shimizu, A., Matsui, I., Sugimoto, N., Wang, W., Bandow, H. and Hatakeyama, S. (2008). Transport and transformation of total reactive nitrogen over the East China Sea. *J. Geophys. Res.* 113: D10306.
- Taniguchi, Y., Shimada, K., Takami, A., Lin, N.H., Chan, C.K., Kim, Y.P. and Hatakeyama, S. (2017). Transboundary and local air pollutants in western Japan distinguished on the basis of ratios of metallic elements in size-segregated aerosols. *Aerosol Air Qual. Res.* 17: 3141–3150.
- Tao, Y., Yin, Z., Ye, X., Ma, Z. and Chen, J. (2014). Size distribution of water-soluble inorganic ions in urban aerosols in Shanghai. *Atmos. Pollut. Res.* 5: 639–647.
- Toppinga, D., Coea, H., McFiggansa, G., Burgessa, R., Allana, J., Alfarrab, M.R., Bowera, K., Choulartona, T. W., Decesaric, S. and Facchinic, M. C. (2004). Aerosol chemical characteristics from sampling conducted on the Island of Jeju, Korea during ACE Asia. *Atmos. Environ.* 38: 2111–2123.
- Uno, I., Carmichael, G.R., Streets, D.G., Tang, Y., Yienger,

- J.J., Satake, S., Wang, Z., Woo, J.H., Guttikunda, S., Uematsu, M., Matsumoto, K., Tanimoto, H., Yoshioka, K. and Iida, T. (2003). Regional chemical weather forecasting system CFORS: Model descriptions and analysis of surface observations at Japanese island stations during the ACE-Asia experiment. *J. Geophys. Res.* 108: 8668.
- Uno, I., Pan, X., Itahashi, S., Yumimoto, K., Hara, Y., Kuribayashi, M., Yamamoto, S., Shimohara, T., Tamura, K., Ogata, Y., Osada, K., Kamikuchi, Y., Yamada, S. and Kobayashi, H. (2016). Overview of long-lasting yellow sand and high concentration of air pollution observed over the northern Kyushu area in late May–early June 2014. *J. Japan Soc. Atmos. Environ.* 51: 44–57 (in Japanese).
- Wilson, W.E. and Suh, H.H. (1997). Fine particles and coarse particles: Concentration relationships relevant to epidemiologic studies. *J. Air Waste Manage. Assoc.* 47: 1238–1249.
- Xia, Y., Zhao, Y. and Nielsen, C.P. (2016). Benefits of China's efforts in gaseous pollutant control indicated by the bottom-up emissions and satellite observations 2000–2014. *Atmos. Environ.* 136: 43–53.
- Yumoto, Y., Shimada, K., Araki, Y., Yoshino, A., Takami, A. and Hatakeyama, S. (2015). Size-segregated chemical analyses of particles transported from East Asia to Cape Hedo, Okinawa and their transformation mechanisms during the transport. *Eaorozoru Kenkyu* 30: 115–125 (in Japanese with English Abstract).
- Zhao, Y. and Gao, Y. (2008). Mass size distributions of water-soluble inorganic and organic ions in size-segregated aerosols over metropolitan Newark in the US east coast. *Atmos. Environ.* 42: 4063–4078.
- Zhuang, H., Chan, C.K., Fang, M. and Wexler, A.S. (1999). Formation of nitrate and non-sea-salt sulfate on coarse particles. *Atmos. Environ.* 33: 4223–4233.

Received for review, December 30, 2016

Revised, June 4, 2017

Accepted, June 5, 2017